

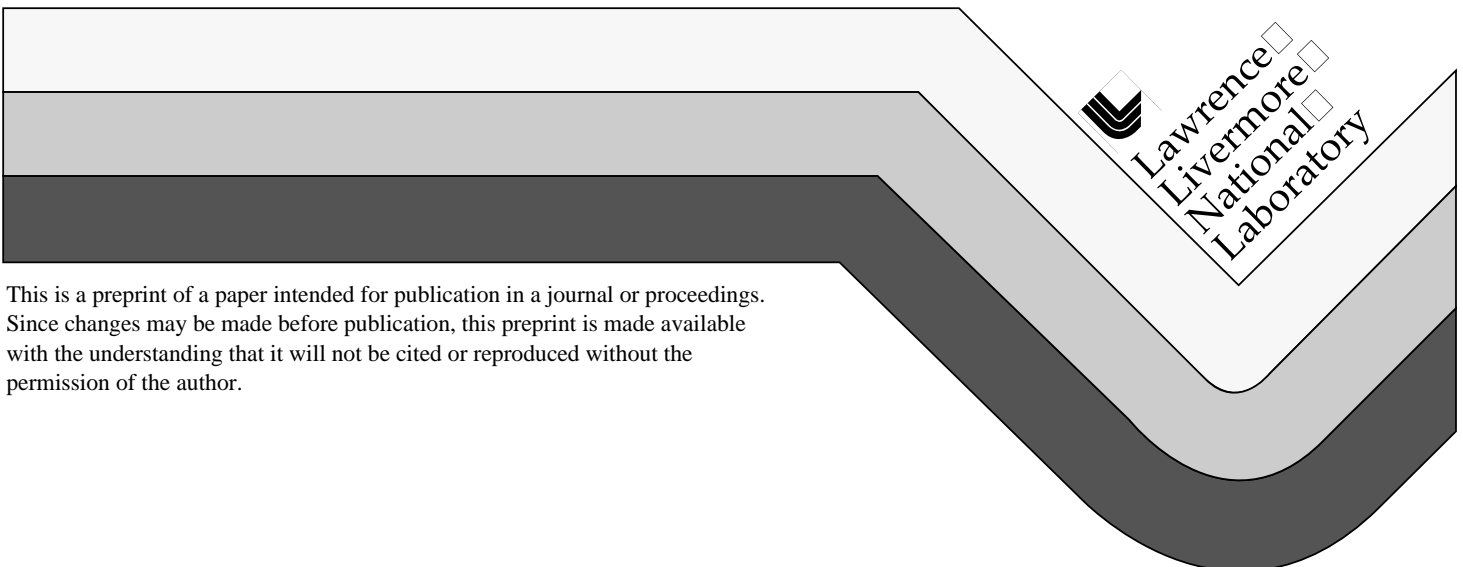
UCRL-JC-131165
PREPRINT

Fatigue and Fracture of Fiber Composites Under Combined Interlaminar Stresses

S.J. DeTeresa
D.C. Freeman
S.E. Groves

This paper was prepared for submittal to the
American Society for Composites 13th Technical Conference
Baltimore, MD
September 21-23, 1998

June 25, 1998



This is a preprint of a paper intended for publication in a journal or proceedings.
Since changes may be made before publication, this preprint is made available
with the understanding that it will not be cited or reproduced without the
permission of the author.

DISCLAIMER

This document was prepared as an account of work sponsored by an agency of the United States Government. Neither the United States Government nor the University of California nor any of their employees, makes any warranty, express or implied, or assumes any legal liability or responsibility for the accuracy, completeness, or usefulness of any information, apparatus, product, or process disclosed, or represents that its use would not infringe privately owned rights. Reference herein to any specific commercial product, process, or service by trade name, trademark, manufacturer, or otherwise, does not necessarily constitute or imply its endorsement, recommendation, or favoring by the United States Government or the University of California. The views and opinions of authors expressed herein do not necessarily state or reflect those of the United States Government or the University of California, and shall not be used for advertising or product endorsement purposes.

Fatigue and Fracture of Fiber Composites Under Combined Interlaminar Stresses*

S. J. DeTeresa, D. C. Freeman, and S. E. Groves
University of California
Lawrence Livermore National Laboratory

ABSTRACT

As part of efforts to develop a three-dimensional failure model for composites, a study of failure and fatigue due to combined interlaminar stresses was conducted. The combined stresses were generated using a hollow cylindrical specimen, which was subjected to normal compression and torsion. For both glass and carbon fiber composites, normal compression resulted in a significant enhancement in the interlaminar shear stress and strain at failure. Under moderate compression levels, the failure mode transitioned from elastic to plastic. The observed failure envelope could not be adequately captured using common ply-level failure models. Alternate modeling approaches were examined and it was found that a pressure-dependent failure criterion was required to reproduce the experimental results. The magnitude of the pressure-dependent terms of this model was found to be material dependent. The interlaminar shear fatigue behavior of a carbon/epoxy system was also studied using the cylindrical specimen. Preliminary results indicate that a single S/N curve which is normalized for interlaminar shear strength may be able to reproduce the effects of both temperature and out-of-plane compression on fatigue life. The results demonstrate that there are significant gains to be made in improving interlaminar strengths of composite structures by applying out-of-plane compression. This effect could be exploited for improved strength and fatigue life of composite joints and other regions in structures where interlaminar stress states are critical.

INTRODUCTION

While the failure due to combined in-plane stresses in fiber composite laminates has been well-studied, little information is available concerning interlaminar failure under combined out-of-plane stresses. Since most common composites do not incorporate reinforcement through the thickness direction, failure under these stresses is solely matrix-dominated. Consequently, it is expected that interactive stress effects exist for these delamination failure modes. In this study, failure under combined through-thickness compression and interlaminar shear was examined under quasi-static and fatigue loading conditions. Practical

*This work was performed under the auspices of the U. S. Department of Energy by Lawrence Livermore National Laboratory under contract No. W-7405-Eng-48.

examples of where this particular combined stress state can occur include; the edges of multidirectional laminates, bonded and bolted joints, and the interior of a laminate under lateral impact. In fact, it has been shown that these stresses occur in the popular short-beam shear test [1]. Until the combined stress effects are known, extracting shear strength values from this test is difficult. Past experience has shown that benefits in interlaminar shear performance of joints can be obtained if there is some mechanism for providing through-thickness compression [2]. Methods which have been developed to provide the enhanced compression included clamping action via bolts and self-generated compression in conical joints for composite cylinders [3].

In order to fully exploit any gains realized under combined interlaminar shear and compression, we have developed a test method to quantify these gains. The only previous work we are aware of are several studies to characterize the failure of glass fiber composites at cryogenic temperatures for application to insulation in the toroidal field coils of the International Thermonuclear Experimental Reactor (ITER) [4] and the Compact Ignition Tokamak (CIT) [5]. In the latter, the strength of laminates tested at several orientations provided a fixed ratio of combined compression and shear, whereas in the former, compression was applied independently in a biaxial test device. However, due to the nature of the test design, interlaminar failure could only be attained under high compression levels. Although both studies revealed an increase in shear strength with compression, neither provided any measure of the stress-strain behavior in the combined stress state.

Study of the fatigue under combined interlaminar shear and compression was also undertaken for the ITER project [6]. Due to the fixed ratio of shear and compression stresses in these tests, it was sometimes difficult to distinguish whether failure was due to shear or compression. To our knowledge, this is the only study of fatigue of fiber composites under combined interlaminar stresses.

EXPERIMENTAL

The specimen we developed for studies of fatigue and failure under combined interlaminar shear and compression is shown in Figure 1. Thick-section composites were machined into small "dogbone" samples having a hollow cylinder gage section. Soon after we started our program, we discovered that this specimen had been used over 20 years earlier to study the uncoupled interlaminar shear and tensile strengths of fiberglass laminates [7]. Our work extends the use of this specimen to study combined stress effects. Future tests will also be performed on composite-metal bonds using a sandwich specimen consisting of two plates of steel bonded with a few plies of fiber composite, which is also shown in Figure 1.

The gage section of the specimens were machined to nominal dimensions of 0.25" long and 0.625" inner and 0.825" outer diameters. The transition from square ends to the cylindrical gage section was made with a 0.25" radius. The 0.625" diameter holes were machined using a carbide drill and these holes served as the

datum for grinding the outside contour and for aligning the specimens in test fixtures.

This specimen is not a thin-walled cylinder and in order to calculate maximum shear stresses from measured torque values, the following well-known equations for both purely elastic and plastic behavior were used:

$$t_e = \frac{2T}{p r_o^3 \left(\frac{r_o^4}{r_i^4} - 1 \right)} \quad (1)$$

$$t_p = \frac{2T}{2p(r_o^3 - r_i^3)} \quad (2)$$

where r_i and r_o are the inner and outer radii, respectively and T is the torque. Torque-twist curves were examined to determine if the behavior at failure was predominantly elastic or plastic and the corresponding equation was used to calculate the shear stress at failure. For this specimen, the maximum error in using either (1) or (2) is only 12%.

All tests were performed using MTS servohydraulic, biaxial test machines capable of controlling both torque or rotation and normal force or displacement. For static strength and fatigue tests, a constant compression force was applied while the specimen was twisted to failure under torque control. Special water-cooled adapter fixtures were built to allow heating using a quartz clamshell oven while maintaining precise concentric and parallel alignment to the specimens. In the fatigue and elevated temperature tests, temperature was monitored using a thermocouple mounted directly to the specimen. Preliminary fatigue tests conducted using 3 and 30 Hz sawtooth waves showed that there were no heating effects at the higher rate and that the lifetimes were identical at the two frequencies. The slower rate was used for the higher stress fatigue tests to allow sufficient time to establish torque control. The lower stress, high-cycle tests were run at 30 Hz. All fatigue tests were conducted at a shear stress ratio of $R = 0.1$.

Four different types of specimens were tested: a $[45/0/-45/90]_{XS}$ laminate of T300 carbon fiber with Hexcel F584 epoxy matrix, a $[0/90]_{XS}$ laminate of IM7 carbon fiber with Hexcel 8551-7 epoxy matrix, a liquid-molded E-glass, plain-weave fabric/vinyl ester laminate, and a filament-wound, $[90_2/\pm 45]_{XS}$ panel of S2-glass/epoxy. All were machined from panels which were nominally 1" thick. The E-glass/vinyl ester composite was kindly donated by Dr. Wayne Phyllaier of the CDNSWC, David Taylor Laboratory. It is typical of the low-cost composite material which is a prominent candidate for primary structures in surface ships.

RESULTS

The shear stress-strain response, as indicated by torque-twist curves, showed both enhanced strength and ductility under constant compression stress. Room temperature curves for the T300/F584, IM7/8551-7 and E-glass/vinyl Ester laminates are shown in Figures 2–4.

The T300/F584 and E-glass/vinyl ester laminates appear to be elastic to failure under pure interlaminar shear. However, under nearly all compression stresses, including relatively low values, the response becomes more noticeably plastic. The increase in strength and ductility continued until compression levels approached the through-thickness compression strength. Cross-ply and quasi-isotropic laminates exhibit high interlaminar compression strengths, thereby allowing significant enhancement of the shear strength through large superimposed compression stresses. While the trends in strength and strain at failure were similar for the materials, there were some differences in the effects of compression on the stress-strain curves. In the E-glass fabric composite, it seemed to have little effect on the shape of the shear stress-strain curve, with nearly all curves falling on top one another. Similar results were obtained for the S2-glass/epoxy laminate. For the T300/F584 laminate, compression caused an increase in stiffness and yielded a surprisingly uniform and high shear failure strain. Although complicated by some settling in the fixture, the response of the IM7/8551-7 laminate shows that compression causes an increase in stiffness, strength and failure strain.

The envelope for shear failure as a function of interlaminar compression for all materials is shown in Figure 5. The failure curves indicate that for the increase in shear strength up to the maximum value, the behavior is quadratic. Attempts to fit this data using well-known composite failure criteria failed due to the inability of these models to capture failure under the high, interlaminar compression stresses achieved in multidirectional laminates. At low compression stress, some of these models do predict the trend toward increased interlaminar shear strength. However, the eventual drop-off in shear strength is predicted to occur at compression stresses which are much lower than observed experimentally.

Because the material response in this combined stress state is matrix-dominated, a yield criterion which has been successfully used for pure polymers was applied to the failure data. The model was first introduced by Hu and Pae [8] and is given by:

$$J_2' = \sum_{i=0}^{\infty} \mathbf{a}_i J_1^i \quad (3)$$

where J_2' is the second invariant of the deviatoric stress tensor, J_1 is the first stress invariant and \mathbf{a}_i are constants. Previous work has shown that expanding (1) to the first two terms in J_1 adequately captures the yield behavior of most polymers. This expression is given by

$$J_2' = \mathbf{a}_0 + \mathbf{a}_1 J_1 + \mathbf{a}_2 J_1^2 \quad (4)$$

Written in this form, a_0 is the square of the interlaminar shear strength under pure shear. Furthermore, because of the confinement imposed on the polymer matrix by the relatively rigid fiber, it was assumed that the resin is in a state of nearly one-dimensional strain. A ply-level stress analysis showed that this assumption was more valid for the carbon laminates than the glass composites.

Only the data for shear strength increasing with normal stress up to the maximum value were fitted using the yield condition. The parameters for the different laminates obtained from the fit of (4) to the strength data in units of ksi are summarized in Table I. The first column of data are the shear strengths under pure interlaminar shear. For the carbon laminates, these are lower than what is normally reported based on the short beam test. It is possible that the part of the discrepancy is due to the problems discussed earlier about interpreting the beam test. The two glass laminates behave similarly in both the linear and second-order rates of increase in shear strength with pressure. The carbon laminates show a much stronger linear dependence on pressure, especially the T300/F584 laminate which exhibited more than a factor of three improvement in shear strength at the highest compression levels. Nearly all materials exhibit the same second-order pressure dependence, as represented by the term a_3 .

Table I. BEST FIT PARAMETERS FOR A SECOND-ORDER, PRESSURE-DEPENDENT YIELD FUNCTION.

Material	$\sqrt{a_0}$	a_1	a_3
S2-Glass Fiber, DER Epoxy	3.58	-1.7	0.032
E-Glass Fiber, Vinyl Ester	7.24	-1.4	0.038
IM7 Carbon, 8551-7	9.71	-3.3	0.035
T300 Carbon, F584 Epoxy	8.39	-5.6	0.033

A preliminary set of fatigue data for the IM7/8551-7 laminate was obtained for the IM7/8551-7 laminates at ambient temperature and 200°F. Additionally, the effect of applying 15 ksi compression during fatigue at 200°F was also examined for a few specimens. All the fatigue lifetimes appear to fit a single S/N curve when stress is plotted as the percentage of the corresponding ultimate shear strength, as shown in Figure 6. This correspondence of normalized fatigue lifetimes at the two temperatures and stresses suggests that the life is limited by a single degradation mechanism. Since compression elevates the shear strength, it appears that it can also significantly extended fatigue lifetimes at a fixed shear stress.

CONCLUSIONS

New results for the fatigue and failure of fiber composites under combined interlaminar stresses were obtained using a cylindrical specimen machined from thick-section panels. The enhancement in shear strength and ductility due to through-thickness compression was quantified for various laminates based on carbon and glass fibers. The carbon systems showed a much stronger increase in shear strength with compression, which was modeled using a pressure-dependent failure criterion. The specimen is also suitable for studying the fatigue under combined stresses and preliminary results were collected for a carbon/epoxy laminate. Now that these beneficial effects of compression on performance in interlaminar shear can be quantified, they can be exploited in application, particularly in the design of durable joints and bonds.

ACKNOWLEDGEMENT

The authors gratefully acknowledge the support by the Office of Naval Research under Contract No. N00014-96-F-0422, technical monitor Dr. Y. Rajapakse, and by the Joint DOE/DoD Technology Development Munitions Program. We also would like to thank Mr. Will Andrade and Mr. Jeff Peterson for developing the machining techniques and preparing the specimens.

REFERENCES

1. Berg, C. A., Tirosh, J., and Israeli, M., "Analysis of Short Beam Bending of Fiber Reinforced Composites," *Composite Materials: Testing and Design (Second Conference)*, ASTM STP 497, American Society for Testing and Materials, pp. 206-218 (1972).
2. Hart-Smith, L. J., "Joints" in **Engineered Materials Handbook, Volume 1: Composites**, ASM International, Metals Park, OH, pg. 490 (1987).
3. Peters, S. T., Humphrey, W. D., and Foral, R. F., "Filament Winding Composite Structure Fabrication," SAMPE, Covina, CA pp. (1991).
4. Simon, N. J., Drexler, E. S., and Reed, R. P., "Shear/Compression Tests for ITER Magnet Insulation," in **Advances in Cryogenic Engineering, Volume 40, Part B**, R. P. Reed, et al., Editors, Plenum Press, NY, pp. 977-983 (1994).
5. McManamy, T. J., Kanemoto, G., and Snook, P., "Insulation irradiation test programme for the Compact Ignition Tokamak," *Cryogenics*, **31** 277-281 (1991).

6. Reed, R. P., Fabian, P. E., and Bauer-McDaniel, T. S., "Shear/compressive fatigue of insulation systems at low temperatures," *Cryogenics*, **35**(11) 685–688 (1995).
7. McKenna, G. B., and Mandell, J. F., and McGarry, F. J., "Interlaminar Strength and Toughness of Fiberglass Laminates," *29th Annual Tech. Conf., Reinforced Plastics/Composites Institute, The Society of the Plastics Industry*, Washington D. C., Section 13-C, pp. 1–8 (1974).
8. Hu, L. W. and Pae, K. D., "Inclusion of the Hydrostatic Stress Component in the Formulation of the Yield Condition," *J. Franklin Inst.* **275** (1963) 491.

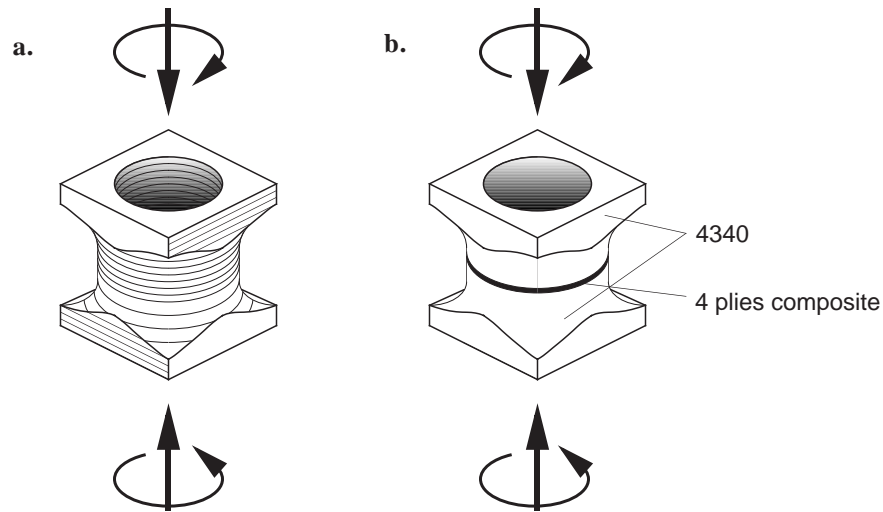


Figure 1. Test specimens for generating combined interlaminar shear/normal stress states. (a) All-composite and (b) 4340 steel sandwich with thin composite layer.

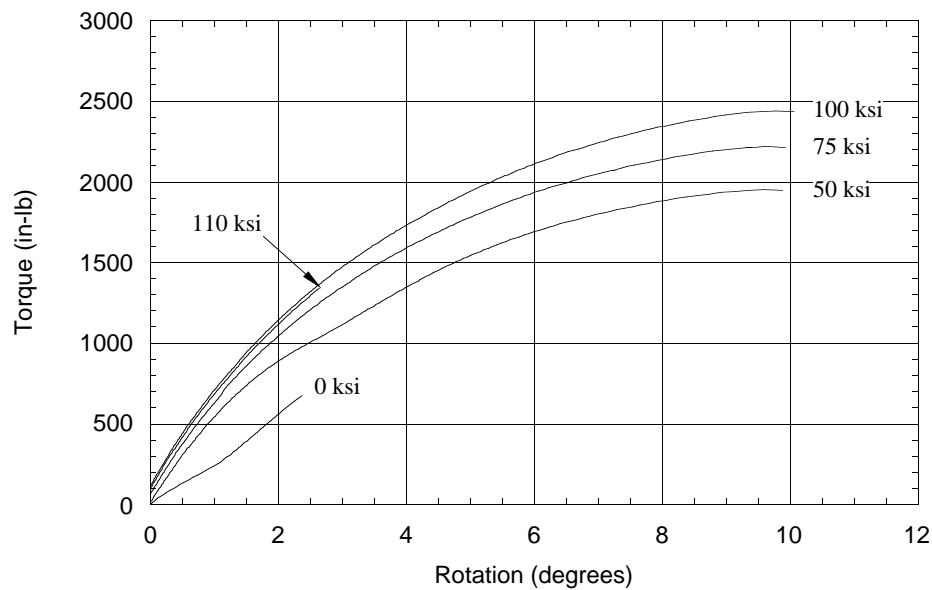


Figure 2. Torque-twist behavior of a T300/F584 quasi-isotropic laminate as a function of through-thickness compression.

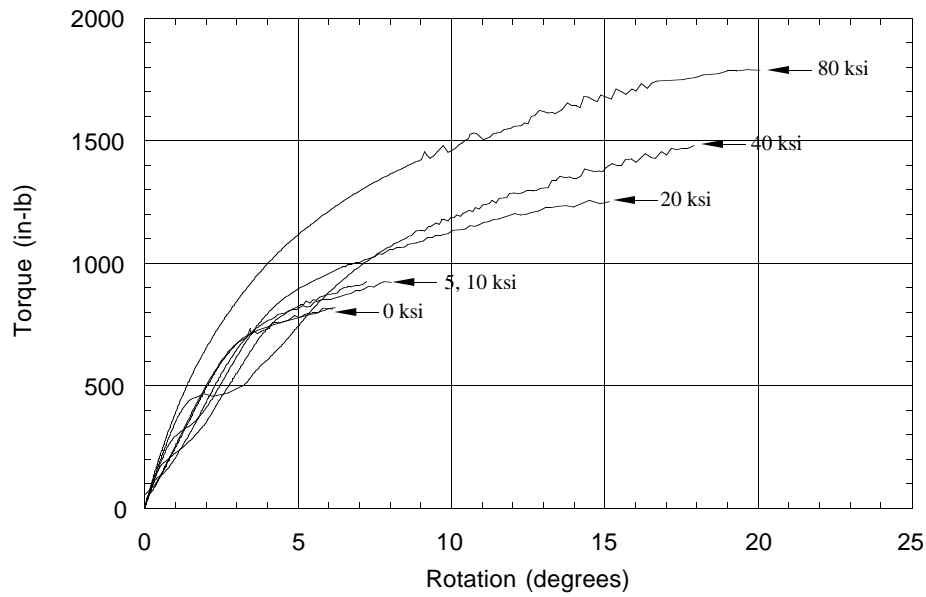


Figure 3. Torque-twist behavior of an IM7/8551-7 cross-ply laminate as a function of through-thickness compression.

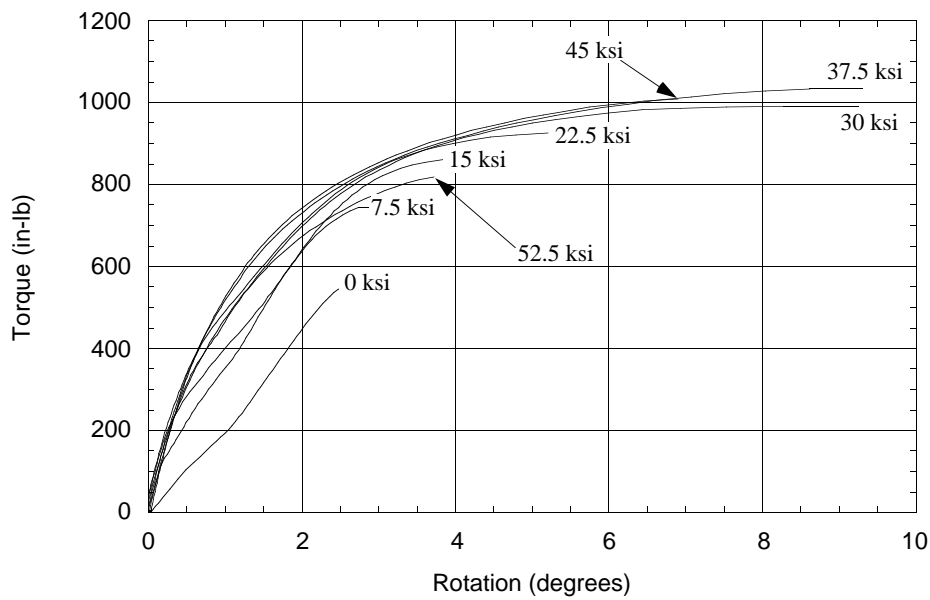


Figure 4. Torque-twist behavior of an E-glass/vinyl ester fabric cross-ply laminate as a function of through-thickness compression.

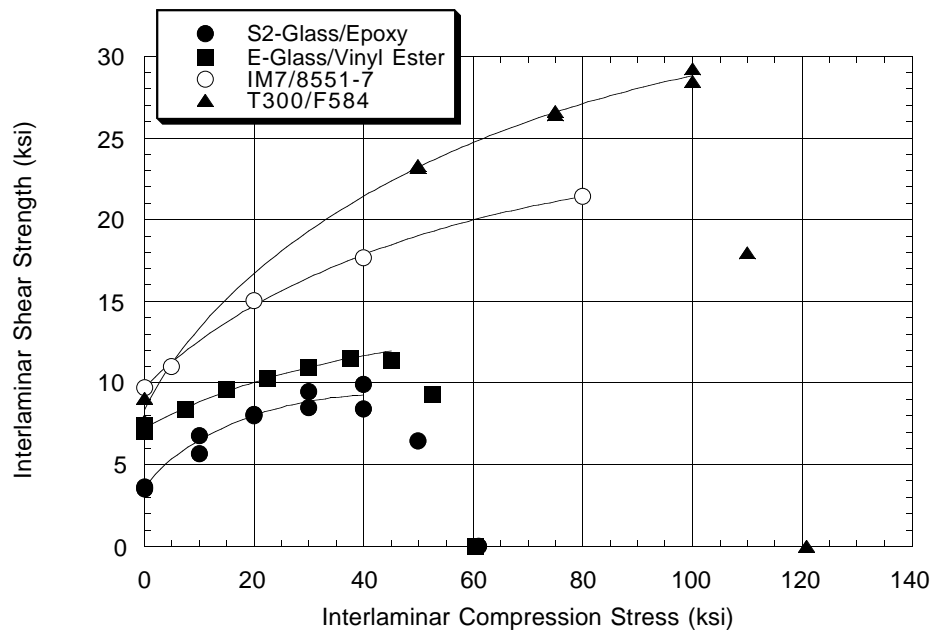


Figure 5. Effect of through-thickness compression on interlaminar shear strength.

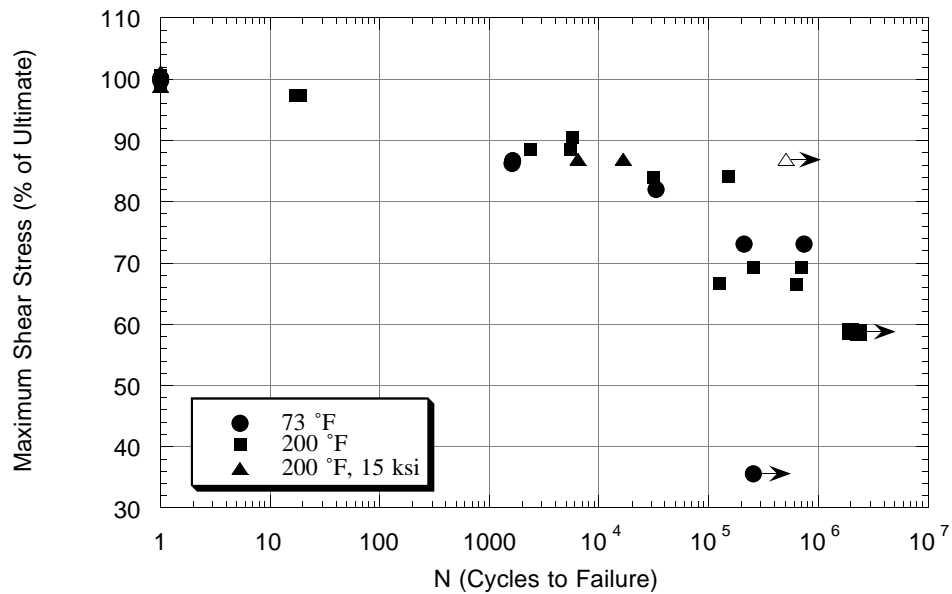


Figure 6. Interlaminar shear fatigue curves for IM7/8551-7 composite (arrows indicate that the specimen did not fail).